

Uncertainty analysis of an SST-2 fusion reactor design

Stuart I. Muldrew^{a,*}, Hanni Lux^a, Vinay Menon^b, Radhakrishnan Srinivasan^b

^a Culham Centre for Fusion Energy, UK Atomic Energy Authority, Culham Science Centre, Abingdon, Oxfordshire OX14 3DB, UK

^b Institute for Plasma Research, Bhat, Gandhinagar 382428, Gujarat, India

ARTICLE INFO

MSC:
00-01
99-00

Keywords:

Fusion reactor
SST-2
Uncertainty quantification
System studies

ABSTRACT

Systems codes assess the viability of fusion reactor designs by using simplified models for the entire reactor system that allow for the exploration of large areas of parameter space. However, every design will have an associated uncertainty that arises from the accuracy of the models used, the assumptions made and the values of input parameters adopted. For individual codes, the uncertainty on their results can be quantified by investigating the dependence on the combination of input parameters. More generally, different codes can be compared against each other to test the underlying models. In this paper we compare the results of two systems codes, SPECTRE and PROCESS, using a conceptual design for the SST-2 fusion reactor for benchmarking. We find that overall both codes produce similar results, however different plasma temperatures and densities are found due to the treatment of radiation in relation to the L-H threshold, and different fusion reaction rates. We then apply a Monte-Carlo based uncertainty quantification tool using PROCESS to find that while the design can produce in excess of 100 MW of fusion power, it is unlikely to produce pulses over 400 s. This is in agreement with previous work and suggests a larger aspect ratio is required.

1. Introduction

Systems codes are a powerful tool for designing the next generation of nuclear fusion reactors. By exploring a large design space in a single calculation, they can obtain highly optimised solutions. However, while a single design is informative, it does not give the whole picture. Often new designs will push boundaries, whether that involves scaling to new physical regimes or applying new technologies. All of this will introduce uncertainty which needs to be quantified to give a complete understanding of the performance of a proposed reactor. Uncertainty analysis and sensitivity studies can then inform about high impact areas, critical design aspects or simply confirm the robustness of the design.

For this study we have used two systems codes, SPECTRE [1] and PROCESS [2,3]. SPECTRE was developed for the Indian DEMO program [1], while PROCESS has been applied to a number of designs, most recently the European DEMO [4]. Both codes solve for the plasma properties and include models for bremsstrahlung, synchrotron and impurity line-radiation. Beyond the plasma properties, PROCESS additionally solves for a number of engineering constraints.

We have chosen to apply the two codes to, and quantify the uncertainty of, a recently published conceptual design for SST-2 (Steady-state Superconducting Tokamak-2) [5]. The SST-2 fusion reactor is a

proposed medium sized device with low fusion gain ($Q = 5$), and capable of producing fusion power from 100 to 300 MW. Tritium breeding will be achieved by having breeding blankets only on the outboard side, while on the inboard side, shielding blankets will be placed due to the limited space available. The magnets will be superconducting in nature to achieve steady-state operation.

The rest of the paper is set out as follows. In Section 2 we benchmark the outputs of SPECTRE and PROCESS using the conceptual design of SST-2. In Section 3 we apply the PROCESS Monte-Carlo uncertainty quantification tool to the design to investigate the variation in fusion power and pulse length. In Section 4 we present our conclusions.

2. Benchmarking between SPECTRE and PROCESS

In order to compare results between SPECTRE and PROCESS, we benchmarked the codes using an updated version of a conceptual design for SST-2 presented in Srinivasan et al. [5]. This was originally produced using SPECTRE. PROCESS has an extensive and detailed output, and for brevity we will restrict our comparison to a few core parameters. These are presented in Table 1. The poloidal cross-section from the PROCESS run is shown in Fig. 1. PROCESS version number 1.0.14-5-g4c4a322 was used.

PROCESS uses an optimiser when solving and for this run we have solved for maximum pulse length (see Section 3 for a discussion). To

* Corresponding author.

E-mail address: stuart.muldrew@ukaea.uk (S.I. Muldrew).

Table 1

Selected parameters for SST-2 produced by SPECTRE and PROCESS. Values marked with IP were given as fixed inputs.

| Parameter | SPECTRE | PROCESS |
|---|------------|------------|
| Major radius, R (m) | 4.42 | 4.42 (IP) |
| Aspect ratio, $A = R/a$ | 3.00 (IP) | 3.00 (IP) |
| Elongation, κ_{95} | 1.70 (IP) | 1.70 (IP) |
| Triangularity, δ_{95} | 0.240 (IP) | 0.240 (IP) |
| Fusion power, P_{fus} (MW) | 100 | 100 |
| Auxiliary power, P_{aux} (MW) | 20.0 | 20.0 |
| Toroidal field, B_T (T) | 5.42 | 5.42 |
| Plasma current, I_p (MA) | 11.2 | 11.2 |
| Safety factor, q_{95} | 3.00 (IP) | 3.00 |
| Normalised beta, β_N | 1.22 | 1.34 |
| Energy confinement time, τ_E (s) | 3.14 | 2.92 |
| H-factor, $H_{IPB98(y,2)}$ | 1.00 (IP) | 1.06 |
| Greenwald fraction, n/n_{GW} | 0.650 (IP) | 0.580 |
| Density weighted temperature, $\langle T_e \rangle_n$ (keV) | 6.09 | 7.70 |
| L-H threshold “Loss” Power (MW) | 29.2 | 25.1 |
| L-H threshold (Snipes [6]) (MW) | 28.1 | 24.1 |
| Neutron wall load (MW m^{-2}) | 0.205 | 0.202 |
| Burn time (s) | – | 207 |

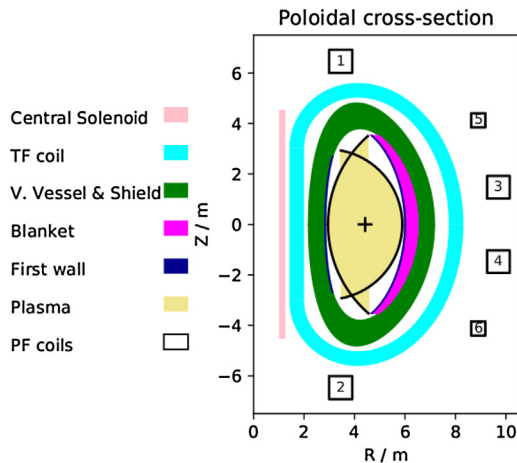


Fig. 1. The poloidal cross-section from the PROCESS output.

produce a solution close to SPECTRE, a number fixed inputs have been applied, as noted in Table 1, and the fusion power has been constrained to a maximum of 100 MW. Both codes use fixed beryllium and argon impurity fractions of 1.8 and 0.21 per cent respectively; for intrinsic and seed impurities which produce radiation that lowers the heat load on the divertor. Overall, PROCESS finds similar performance parameters; with the fusion power, auxiliary power, toroidal magnetic field, safety factor and plasma current all the same. Differences however start to appear in the plasma properties.

PROCESS adopts a lower density and higher temperature compared to SPECTRE. β_N is additionally higher. The lower density yields a lower confinement time for PROCESS, with both codes using the IPB98(y,2) scaling law [7]. PROCESS boosts the confinement time from the scaling with a higher H-factor, however the overall confinement time is still lower. These differences arise because SPECTRE and PROCESS use different fusion reaction rates and have different implementations of the L-H threshold.

The fusion power is given by the product of the deuterium and tritium densities, the energy released by the reaction and the cross-section averaged over the relative velocities (the reaction rate). For SPECTRE the reaction rate is given by a simple relation to electron temperature (Eq. (4.2) of [1]). For PROCESS the reaction rate is calculated by integrating over the plasma profile using rate constants from Bosch and

Hale [8]. This will lead to potentially different fusion powers being calculated. A detailed study comparing the two methods is beyond the scope of this paper and will be considered in future work.

The main cause of the differences between SPECTRE and PROCESS is the implementation of the L-H threshold. Both codes require a “loss” power to be above an L-H threshold power for H-mode operation. By default SPECTRE uses the scaling presented in Snipes et al. [6] to obtain the threshold power. PROCESS has a number of L-H threshold scalings implemented, but by default uses that of Martin et al. [9]. To aid benchmarking with SPECTRE, we have implemented the Snipes et al. scaling in PROCESS.

The two scaling relations produce very different threshold powers for the same input values. For the PROCESS solution in Table 1, the L-H threshold power is 24 MW for the Snipes et al. scaling and 34 MW for the Martin et al. scaling. The exact power required is uncertain due to the scatter in the data that the scaling relations are derived from, and the effect of hysteresis. The L-H transition typically occurs at a higher threshold power than the H-L transition, and in practical machine operation H-mode is usually entered at lower density than the target flat-top scenario, as this requires lower transition power. Once in H-mode the density is then increased [9], and this is not captured within either code. For the purpose of this benchmarking we will use the Snipes et al. scaling in both codes, to agree with the original SPECTRE design. However it should be noted that Verdoolaege and Noterdaeme [10] indicate that Martin et al. is a better fit to the H-mode threshold database.

For the same L-H threshold scaling in SPECTRE and PROCESS, different solutions are found because the “loss” power, which is required to be above the threshold, is calculated differently between the codes due to the treatment of radiation. The “loss” power is given by:

$$P_L \equiv P_{in} - dW/dt = P_\alpha + P_{charge} + P_{ohm} + P_{aux} - P_{rad} \quad (1)$$

where P_α is the alpha power, P_{charge} is the non- α charged particle power, P_{ohm} is the Ohmic power, P_{aux} is the auxiliary power, and P_{rad} is the radiation power that is different between the codes. SPECTRE only subtracts the core radiation and so is requiring the loss power from the confinement time scaling to be above the threshold, which it equates to the power crossing the separatrix. PROCESS subtracts all the radiation and so is requiring the power crossing the separatrix to be above the threshold, which is different to the confinement loss power. Therefore the different interpretation of the change in the plasma stored energy between the codes leads to PROCESS being closer to the L-H threshold than SPECTRE, which results in it adopting a different density and temperature to stay above the limit.

3. Uncertainty quantification

PROCESS has a Monte-Carlo based uncertainty quantification tool that has previously been applied to the pre-conceptual design of the European DEMO [11]. For a given parameter, the user specifies a distribution that describes the uncertainty on that parameter. Currently the distributions available are a Gaussian, a lower or upper half-Gaussian or a uniform distribution. Having specified the centre and width, values for the parameter are drawn at random using the distribution. This is done for all the parameters with uncertainty, which are combined into a single input, and run with PROCESS. Parameters chosen to be used in the uncertainty quantification must have fixed values in the input. The generation of inputs is repeated a user-specified number of times and the variation of outputs between runs is used to quantify the uncertainty.

The following parameters and distributions were used to evaluate the uncertainty on the SST-2 conceptual design. They were chosen based on areas of uncertainty identified in our models and more detail can be found in Lux et al. [11]:

Lower bound on the Greenwald density [12]: The minimum density was limited to produce a solution closer to [5], however

PROCESS produces longer pulses for a lower Greenwald fraction. Therefore we apply a lower half-Gaussian to the limit, peaking at 0.58 with a standard deviation of 0.1, reaching the density of optimal pulse.

Upper bound on H-factor: While an H-factor of 1.06 was used for benchmarking, it is possible that a future device could achieve an enhancement. Therefore we have fixed the upper limit on the H-factor using an upper half-Gaussian with standard deviation 0.1 peaking at 1.06.

Core radius in radiation corrected τ_E scaling: PROCESS considers radiation from the core as an instantaneous loss and subtracts this from the loss power in the confinement scaling. The size of the core region will influence the amount of radiation subtracted, so we have taken a Gaussian centred on a normalised radius of 0.75 with a standard deviation of 0.15.

L-H threshold: As discussed in Section 2, the L-H threshold is uncertain. We have applied a uniform distribution between the Snipes et al. value and 1.5 times this, which corresponds to the Martin et al. value from Section 2.

Bootstrap fraction multiplier: PROCESS calculates the bootstrap fraction using the method described in [13]. The uncertainty on this is taken as a Gaussian with standard deviation 0.1.

Current drive efficiency: The current drive is calculated from the NBI and the uncertainty is taken as a Gaussian with fractional standard deviation of 0.05. Note that the runs in Figs. 2 and 3 do not have current drive, and this is only used in the upcoming case where we explicitly state it.

Ejima coefficient: The Ejima coefficient is used to calculate the flux consumption and influences the pulse length. Here we have taken a Gaussian centred on 0.35 with a standard deviation 0.05.

We generated 1000 realisations and ran with PROCESS. Initially we allowed for no current drive from the NBI to agree with the original SPECTRE run and increased the upper limit on the fusion power from 100 MW to 300 MW. The radial build was fixed to values obtained in Section 2 so that just performance parameters are being tested.

We have chosen to focus our analysis on the fusion power and pulse length. SST-2 should operate in the 100 to 300 MW fusion power range. It is an additional aspiration that it should have ITER-like pulse lengths, with a target of 400 s. However it is already known that the flux linkage of current design is too low to achieve a 400 s pulse [5]. SPECTRE does not calculate pulse lengths and no estimate of the current design's pulse length has been made. PROCESS does calculate pulse length and using our uncertainty analysis will help inform what design changes need to be

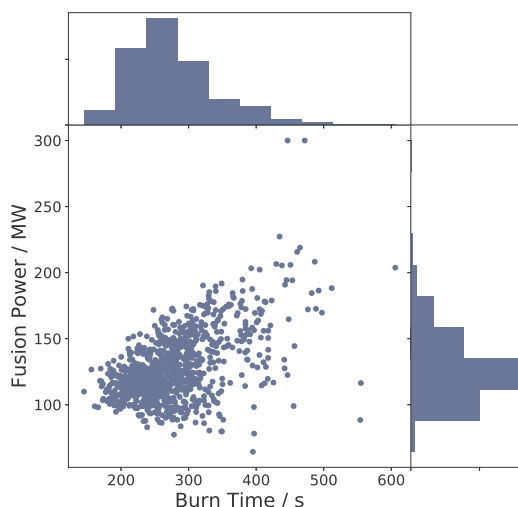


Fig. 2. The uncertainty in the fusion power to burn time for no auxiliary current drive. PROCESS optimised for pulse length.

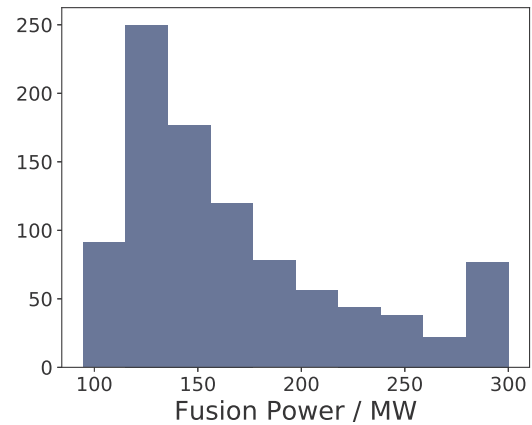


Fig. 3. The distribution of fusion power when optimised for fusion gain.

made.

Fig. 2 shows the fusion power against burn time. The majority of solutions are clustered with burn times between 200 and 350 s, and fusion power between 100 and 150 MW. At the extremes of the uncertainty distributions, fusion power as high as 300 MW and burn times approaching 600 s can be achieved; while at the other end 11 per cent of cases are below the minimum required fusion power of 100 MW. For this run PROCESS is solving for maximum burn time as opposed to maximum fusion power, therefore higher average fusion powers are possible. Only 5 per cent of the solutions have pulses longer than 400 s which confirms the finding that the current design cannot produce ITER-like pulses. One way of increasing the pulse length is to allow current drive from the NBI, reducing the amount needing to be induced by the central solenoid.

For the reference design optimised for pulse length, PROCESS determines that it is optimal for 10 per cent of the plasma current to be generated by current drive from the NBI. A similar scatter to Fig. 2 is found with current drive, however the burn times are shifted to higher values. The peak of the distribution is approximately 50 s longer than the case with no current drive, however this is still too short suggesting that a change in aspect ratio is required.

We can also run PROCESS optimising for fusion gain instead of pulse length. Fig. 3 gives a histogram of fusion power for this case. It can be seen that the mean of the fusion power distribution peaks 42 MW higher for this design, at the expense of pulse length. Higher fusion power could potentially be obtained by adjusting the radial build, which is not done here. Further design changes need to be made if high power operation approaching 300 MW is required.

Finally we can characterise the impact of each uncertainty using jackknife resampling. The mean and standard deviation of the fusion power and pulse length distributions were determined, and then we reran the uncertainty analysis each time removing one of the uncertainties. The shift in the new mean and standard deviation can be used to determine the impact of each uncertainty. We found that the H-factor (mean shift -47 s) and Ejima coefficient (+37 s) had the largest impact on pulse length, while the lower limit on the density had a smaller effect (-3 s), and the other parameters had no effect. For fusion power the H-factor (-26 MW) and lower limit on the density (+22 MW) had an effect, while the other uncertainties did not.

4. Conclusions

We have benchmarked the outputs of two system codes, SPECTRE and PROCESS, using a conceptual design for the SST-2 fusion reactor. We found that both codes produce broadly similar results, however different fusion reaction rates, and the treatment of radiation in relation to the L-H threshold, leads to different temperatures and densities. PROCESS subtracts the total radiation when calculating the “loss” power for the L-

H threshold, while SPECTRE subtracts just the core radiation. This leads to PROCESS being closer to the L-H threshold.

We then applied a Monte-Carlo based uncertainty quantification tool using PROCESS to the design. We found that 89 per cent of cases produce in excess of 100 MW of fusion power. However the pulse length is unlikely to be in excess of 400 s, agreeing with previous work. This suggests that the aspect ratio needs to be increased to accommodate a larger central solenoid, or alternatively adding high-field HTS inserts into the central solenoid to boost the available flux swing. The highest impact uncertainties were the H-factor, Ejima coefficient and the lower limit on the density, and these should be considered carefully in future designs.

Acknowledgements

The authors wish to thank Michael Kovari for useful discussions. To obtain further information on the data and models underlying this paper please contact PublicationsManager@ukaea.uk.

References

- [1] V. Menon, et al., Physics design and analysis code SPECTRE for tokamak based fusion reactors, 25th IAEA Fusion Energy Conference (2014).
- [2] M. Kovari, et al., “PROCESS”: a systems code for fusion power plants – Part 1: Physics, Fusion Eng. Des. 89 (12) (2014) 3054–3069.
- [3] M. Kovari, et al., “PROCESS”: a systems code for fusion power plants – Part 2: Engineering, Fusion Eng. Des. 104 (2016) 9–20.
- [4] R. Wenninger, et al., The physics and technology basis entering European system code studies for DEMO, Nucl. Fusion 57 (1) (2017) 016011.
- [5] R. Srinivasan, Design and analysis of SST-2 fusion reactor, Fusion Eng. Des. 112 (2016) 240–243.
- [6] J.A. Snipes, et al., Latest results on the H-mode threshold using the international H-mode threshold database, Plasma Phys. Control. Fusion 42 (5A) (2000) A299.
- [7] ITER Physics Expert Group on Confinement, et al., Chapter 2: Plasma confinement and transport, Nucl. Fusion 39 (12) (1999) 2175.
- [8] H.-S. Bosch, G. Hale, Improved formulas for fusion cross-sections and thermal reactivities, Nucl. Fusion 32 (4) (1992) 611 Erratum: Nucl. Fusion 33 (12) (1993) 1919.
- [9] Y.R. Martin, et al., Power requirement for accessing the H-mode in ITER, J. Phys.: Conf. Ser. 123 (1) (2008) 012033.
- [10] G. Verdoolaege, J.-M. Noterdaeme, Robust scaling in fusion science: case study for the L-H power threshold, Nucl. Fusion 55 (11) (2015) 113019.
- [11] H. Lux, et al., Uncertainties in power plant design point evaluations, Fusion Eng. Des. 123 (2017) 63–66.
- [12] M. Greenwald, et al., A new look at density limits in tokamaks, Nucl. Fusion 28 (12) (1988) 2199.
- [13] O. Sauter, C. Angioni, Y.R. Lin-Liu, Neoclassical conductivity and bootstrap current formulas for general axisymmetric equilibria and arbitrary collisionality regime, Phys. Plasmas 6 (7) (1999) 2834–2839.